The Aggregation Behavior of Butyllithium in Diethyl Ether in the Presence of LiBr, $LiClO_4$, and Phenyllithium: A Deuterium-Induced Secondary ^{6}Li-NMR Isotope-Effect Study[1])

by **Bernd Böhler** and **Harald Günther***

Fakultät IV, OC II, University of Siegen, D-57068 Siegen (e-mail: guenmr@chemie.uni-siegen.de)

Dedicated to Professor Dr. *Wolfgang Lüttke* on the occasion of his 95th birthday

The aggregation of BuLi (LiR) in diethyl ether (Et_2O) in the presence of LiBr was studied by ^{6}Li- and ^{13}C-NMR spectroscopy. For a 1.0 : 0.8 mixture of both species, the clusters $(LiR)_4$, Li_4R_3Br, $Li_4R_2Br_2$, Li_4RBr_3, and/or Li_2RBr in the ratio 7 : 81 : 12 with Li_4RBr_3 and/or $Li_2RBr < 1$ were detected with the *isotopic fingerprint method* that is based on secondary deuterium (D)-induced isotope shifts for δ(Li). The raising content of bromide ions causes increased shielding for δ(Li). As in the case of a 1 : 1 MeLi/LiBr mixture in Et_2O, cluster Li_4R_3Br is the most stable one. In the presence of *N*,*N*,*N*′,*N*′-tetramethylethylenediamine (TMEDA), only a mixed dimer was found. For $LiClO_4$, no inclusion of the ClO_4^- ion could be detected. A mixture BuLi/PhLi 1 : 1 in Et_2O in the presence of TMEDA showed only dimers with the mixed dimer as the most stable cluster. Chemical exchange of Li between the two homodimers was detected by EXSY spectroscopy. This implies an exchange mechanism with a *fluxional* tetramer as intermediate.

Introduction. – One of the most important properties of organolithium compounds – valuable intermediates in organic syntheses – is their aggregation tendency in ethereal and hydrocarbon solvents. NMR Spectroscopy plays since long a major role in the structural investigations of these complexes [2]. While earlier information about the degree of aggregation was obtained from colligative properties such as diffusion constants, vapor pressure or freezing point lowerings [3], NMR studies provide more direct evidence for the size and properties of aggregates like dimers, tetramers, or hexamers. In the beginning, the measurement of scalar ^{6,7}Li,^{13}C coupling constants at the lithiated C-atom, pioneered by *Fraenkel* [2f][4] and *Seebach* [5a], yielded important data about aggregate size and aggregate dynamics. The use of the more 'NMR-friendly' isotope ^{6}Li with its small quadrupolar moment (-8.08×10^{-4} barn), which is today the preferred nucleus, led to the empirical *Eqn. 1* [5]:

$$^1J(^{13}C,^6Li) \approx (17 \pm 2)/n \quad (1)$$

that relates the aggregation state, n, ($n = 1$ for a monomer, 2 for a dimer, *etc.*) of a *static* complex, where *inter*- and *intra*-aggregate exchange processes are slow on the NMR timescale, with the magnitude of the scalar ^{13}C,^{6}Li coupling constant that depends on

[1]) NMR Spectroscopy of Organolithium Compounds, Part XXX; for Part XXIX, see [1].

the number of ^{13}C,^{6}Li contacts and decreases for *fluxional* aggregates with *intra*-aggregate exchange processes. Later, chemical-shift *multiplet*s – *isotopic fingerprints* – resulting from deuterium (^{2}H)-induced isotope effects on $\delta(^{6}Li)$ were established as a useful analytical tool [6], and more recently the measurement of diffusion coefficients by DOSY spectroscopy led to promising results [7], especially since it also yields through the magnitude of the diffusion coefficients information about the solvent cage of the particular complex that is not available from other spectroscopic techniques.

Apart from homo-aggregation, the aggregation tendency of Li organics leads to the formation of mixed aggregates if Li salts are present, either as by-products of Li/halogen exchange reactions that are used for the synthesis of the Li reagents, or if inorganic salts are added in order to influence the reaction behavior [2g][8][9]. Structural information about these mixed aggregates is thus important for detailed experimental and/or theoretical mechanistic studies of the reactions of organolithium compounds.

We and others have before reported on the aggregation behavior of MeLi in the presence of LiBr and LiI in Et_2O and THF [9–11], where we characterized mixed tetramers by the isotopic fingerprint method [6][10]. In the present communication, we extend these investigations with a study of the aggregation behavior of BuLi – perhaps the most important organolithium compound in the field of organic synthesis – in Et_2O in the presence of LiBr without and with *N*,*N*,*N*′,*N*′-tetramethylethylenediamine (TMEDA) as an additional ligand. Also, the formation of mixed aggregates with the ClO_4^- anion, and the aggregation between BuLi and PhLi in the presence of TMEDA were examined. In the latter case, it was of interest if aggregate formation is governed by statistics or if certain aggregates are preferred.

Results. – *The System BuLi/LiBr* (1.0:0.8) *in Et₂O.* Based on findings for MeLi/LiBr mixtures [9–11] and the earlier literature [12], we can assume dominating tetramer formation with varying substitution of Bu groups by Br^-. This leads to aggregates or clusters drawn in idealized manner in *Fig. 1*[2]). As we shall show in the following, this assumption is verified by the ^{6}Li- as well as the ^{13}C-NMR spectra also for the present investigation. In addition, the LiBr aggregates $(LiBr)_2$ or $(LiBr)_4$, or a dimer⇌tetramer equilibrium between these two clusters is expected [9][14].

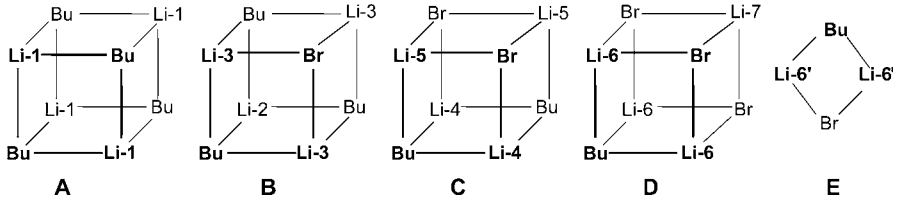

Fig. 1. *Possible aggregates of BuLi/LiBr mixtures*

[2]) The cubic structure shown is based on powder diffraction data for solid MeLi [13]. It is clear that the symmetry of cluster **A** is strongly distorted in the remaining clusters by the increasing introduction of Br^- ions (see, *e.g.*, the DFT-calculated mixed tetramers between MeLi and LiBr [11])

In general, at room temperature all aggregates or clusters are in fast chemical exchange. Lowering the temperature, first *inter*-aggregate and later *intra*-aggregate exchange processes can be slowed down until they do not affect the NMR spectrum. In this case, the complex is called *static*. If only *inter*-aggregate exchange is eliminated with respect to the NMR time-scale and *intra*-aggregate exchange still prevails, we speak of *fluxional* aggregates.

Starting with cluster **A** as the pure tetramer $(BuLi)_4$, different environments for Li^+ then result by increasing replacement of Bu groups by Br^-. With next neighbors for static aggregates collected between brackets and remote neighbors outside the brackets, we expect the Li species compiled in *Table 1*. For *fluxional* aggregates, a time-averaged contact between Li and all ligands, next and remote ones, of the particular cluster exists.

Table 1. *Expected Li Environments in BuLi/LiBr Clusters Shown in* Fig. 1 [a])

Cluster	Li Environment [b])	Occurence
Tetramers		
A	Li-1[CH_2,CH_2,CH_2,]CH_2	4
B	a) Li-2[CH_2,CH_2,CH_2]Br	1
	b) Li-3[CH_2,CH_2,Br]CH_2	3
C	a) Li-4[CH_2,CH_2,Br]Br	2
	b) Li-5[CH_2,Br,Br]CH_2	2
D	a) Li-6[CH_2,Br,Br]Br	3
	b) Li-7[Br,Br,Br]CH_2	1
Dimer		
E	Li-6′[CH_2,Br]	2

[a]) In addition $(LiBr)_2$ and/or $(LiBr)_4$. [b]) Next neighbors in brackets.

The proton-decoupled ^{6}Li-NMR spectrum obtained for a Bu^{6}Li/^{6}LiBr mixture (1.0 : 0.8) at 58.9 MHz and 162 K is shown in *Fig. 2, a*. It was recorded with inverse-gated ^{1}H decoupling [15] in order to avoid signal-intensity distortions due to nuclear *Overhauser* effects (NOEs) [6] and shows, aside from a few smaller signals as, *e.g.*, *2*, six major lines. For the application of the isotopic fingerprint method for signal assignments [6], the principle of which is shortly reviewed in [2c] and in the *Exper. Part*, we prepared a 1.0 : 0.7 : 2.0 mixture of Bu^{6}Li, [α,α-D_2]Bu^{6}Li, and ^{6}LiBr. The CD_2 group then leads to geminal isotope shifts, $^2\Delta(^{2/1}H)^6Li$, in the order of 5 to 10 ppb (!) for directly attached ^{6}Li nuclei. Isotope shifts induced by remote neighbors are usually much smaller and can in most cases be neglected. The signals or fingerprints were then observed in the ^{6}Li-NMR spectrum recorded under the same conditions as the spectrum shown in *Fig. 2, a* (^{1}H decoupling, 162 K) and are reproduced in *Fig. 2, b*. The smaller signals between 0 and 0.35 ppm that are not labelled are assigned to unknown impurities. Their intensities varied for different sample preparations, and they showed no isotope effect. Chemical-shift and isotope-effect data are collected in *Table 2*.

We start our analysis with signals *1* and *7*. The chemical shift of signal *1* is close to that of the external reference LiBr and can thus be attributed to a LiBr cluster. For

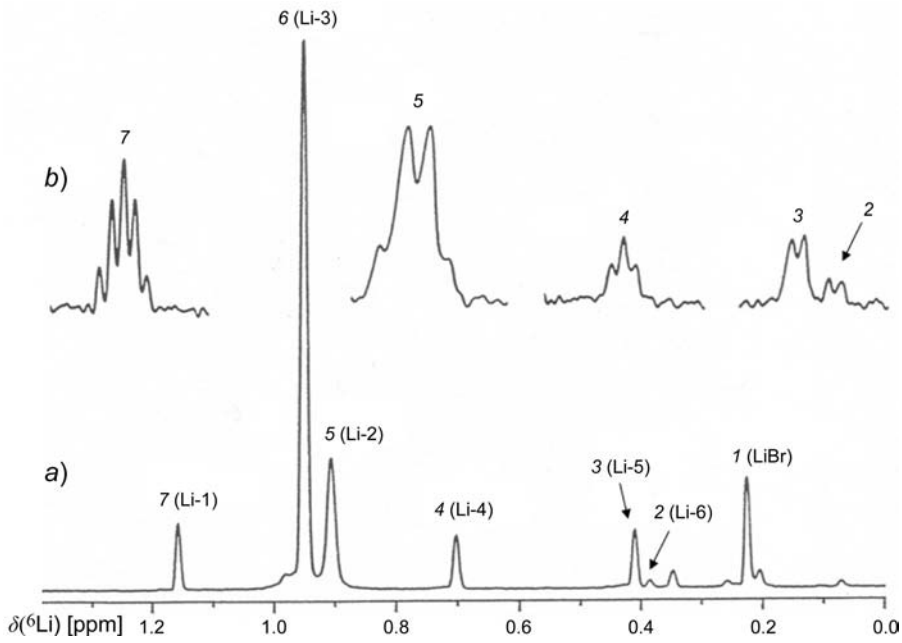

Fig. 2. a) *58.9-MHz Inverse-gated $^{6}Li\{^{1}H\}$-NMR spectrum of $Bu^{6}Li/^{6}LiBr$* (1.0:0.8) *0.44*M *in Et_2O/$(D_{10})Et_2O$ 4:1 at 162 K*. δ-Scale relative to external LiBr 0.1M in [D_8]THF; signal assignments are given above for Li in aggregates **A**–**E**; signals of individual aggregates are *7* (**A**), *5*, *6* (**B**), *3*, *4* (**C**), and *2* (**D** or **E**). b) *Isotopic fingerprints observed in the $^{6}Li\{^{1}H\}$ NMR spectrum of a 1.0:0.7 mixture of $Bu^{6}Li$ and $[\alpha,\alpha-D_2]Bu^{6}Li$ 0.35*M *in the presence of 1 equiv. LiBr in $Et_2O/[D_{10}]Et_2O$* (4:1) *at 156 K*

Table 2. *^{6}Li Chemical Shifts* δ [ppm] *Relative to External LiBr in THF and ^{2}H-Induced Isotope Effects $^{2}\Delta(^{2/1}H)^{6}Li$/ppb*[a]) *of Spectra* a) *and* b) *of* Fig. 1, *Respectively*

Signal	*1*	*2*	*3*	*4*	*5*	*6*	*7*
$\delta(^{6}Li)$	0.22	0.38	0.41	0.70	0.91	0.95	1.16
Assignment	LiBr	Li-6	Li-5	Li-4	Li-2	Li-3	Li-1
$^{2}\Delta(^{2/1}H)^{6}Li$	–	−7.5	−7.5	−6.8	−12.7	>|5.8|	−8.5
Multiplicity	*singlet*	*doublet*	*doublet*	*triplet*	*quadruplet*	–[b])	*quintuplet*

[a]) ^{2}H-Induced isotope effects over two bonds on $\delta(^{6}Li)$, $^{2}\Delta(^{2/1}H)^{6}Li$, are high-frequency shifts and have, therefore, a negative sign, if we define $^{n}\Delta$ by $\delta(h)-\delta(d)$, where $\delta(d)$ is the chemical shift of ^{6}Li in the deuterated compound; for the isotopic fingerprints, only the absolute value is important. [b]) Not resolved.

signal *7* at highest frequency, we observe in *Fig. 1, b*, a 1:4:6:4:1 *quintuplet* that characterizes the corresponding complex as a *fluxional* tetramer where Li has contact with four Bu groups with α-CH_2 and α-CD_2 in the statistical ratio (see *Exper. Part*). Signal *7* is thus due to cluster **A**. In general, for fast *intra*-aggregate exchange the number of NMR signals, n, is correlated with the number c of ligands by $n = c + 1$; for signal *7*, we have $n = 4 + 1 = 5$.

The remaining five signals, *2*–*6*, are due to clusters that contain Br^-. According to *Table 1*, however, if these aggregates were also *fluxional* with fast *intra*-aggregate exchange of neighboring and remote ligands, we would expect only four signals for clusters **B**–**E** of *Fig. 1* instead of five, because in this case the difference between environments labelled *a* and *b* in *Table 1*, *i.e.*, the difference between next and remote neighbors, would vanish. Signals *2* to *6* must, therefore, be attributed to static aggregates where, on the NMR time-scale, all NMR-active dynamic processes are eliminated. In other words, the barrier for *intra*-aggregate exchange in these aggregates is higher than in cluster **A**. They are already in the slow exchange region, while **A** is still in fast exchange. The larger linewidth that we observe for the isotopic fingerprints of signals *2* to *6* as compared to that of signal *7* supports this interpretation: it indicates that the *intra*-aggregate dynamic for signals *2* to *6* is still not fully 'frozen' with the consequence of residual line-broadening. Furthermore, we see that the rate for *intra*-aggregate exchange is apparently slowed down by the inclusion of Br^-.

For the static aggregates of signals *2* to *6*, the isotopic fingerprints represent next neighbor or local environments [16] which may come from different clusters. For the analysis, we expect ^{6}Li shielding caused by the introduction of Br^- due to the well-known heavy atom effect [17]. We thus assume an increasing number of Br^- ions in going from signal *7* to *1*.

The small shift difference between signals *6* and *5* indicates that they belong to lithium environments with the same number of Br^- ions. We can assign Li-2 of cluster **B** with three neighboring CH_2 groups to signal *5* at 0.91 ppm, because we find a *quadruplet* in *Fig. 2, b*, while Li-3 of cluster **B** with the environment [CH_2,CH_2,Br] should give rise to signal *6* at 0.95 ppm. The relative intensity ratio *5*/*6* of 1:3 (see also *Fig. 3*) supports this assignment, however, the expected *triplet* for the isotopic fingerprint of signal *6* could not be resolved. From the measured half-width of 0.68 Hz (=11.5 ppb), we estimate the isotope shift as $<$5.8 ppb, *i.e.*, smaller than the shifts observed for the other signals (*cf. Table 2*). In addition, the line-broadening mentioned above masks the expected fine structure. Surprisingly, we note that the shielding effect for the ^{6}Li resonance due to the introduction of Br^- ion is similar for the directly attached atom Li-3 and for Li-2 at the corner opposite to the halogen. This contrasts with our finding for MeLi/LiBr mixtures [10] where the corresponding Li-2 signal was found close to that of Li-1 (1.80 and 1.72 ppm, resp.). Apparently, the larger size of the Bu group as compared to the Me group leads to different shielding mechanisms.

Signal *4* (δ 0.7) is shifted to lower frequency and shows a fingerprint *triplet*. It can thus be assigned to Li-4 of cluster **C**, if we consider again a shielding effect by Br^- at the opposite corner. Compared to the situation in MeLi/LiBr, Li-4 is now more shielded by 0.34 ppm (1.04 *vs.* 0.70 ppm). Signal *3* than stems from Li-5 of cluster **C** with the environment [CH_2,Br,Br] and the expected *doublet* as fingerprint. Its shift is similar in both systems, MeLi/LiBr and BuLi/LiBr (0.44 *vs.* 0.41 ppm). The assignments derived here are supported by the intensity ratio *4*/*3* of 1:1 (see also *Fig. 3*).

A minor signal *2* close to signal *3* to lower frequency shows a *doublet* in *Fig. 2*, *b*, and could thus arise from Li-6 in cluster **D**. Li-7 of this cluster then coincides with signal *1* of the LiBr cluster or gives rise to one of the small signals around signal *1*. However, the shielding effect of Br^- ion at the opposite corner is missing, otherwise the resonance of

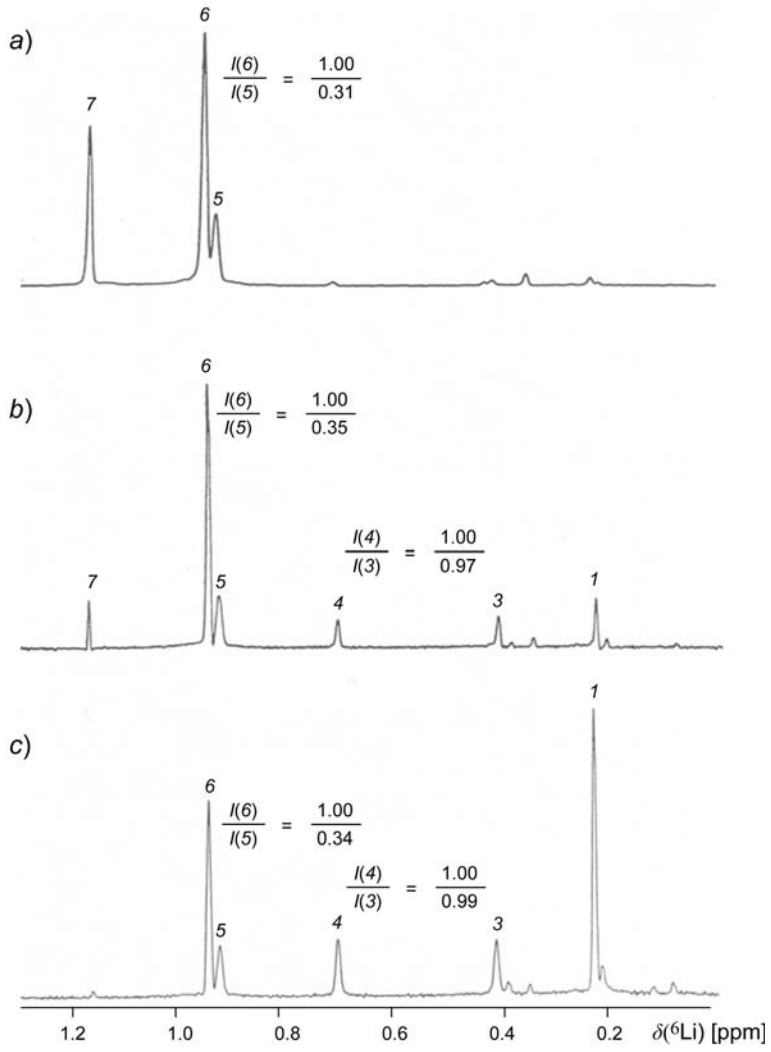

Fig. 3. *^{6}Li{^{1}H}-NMR Spectra of Bu^{6}Li/^{6}LiBr mixtures with different mixing ratios at 166 K:* a) *1.0 : 0.2,* b) *1.0 : 0.8, and* c) *1.0 : 2.0*

Li-6 should appear at even lower frequency. Its ^{6}Li chemical shift (0.38 ppm), however, is close to that of the corresponding ^{6}Li signal in MeLi/LiBr (0.30 or 0.28 ppm [10]). A simple mixed dimer **E** could also explain the fingerprint of signal *2*, then assigned to Li-6′, and the missing shielding effect of the Br^{-} ion from the opposite corner would find an explanation.

From the signal intensities in *Fig. 2, a*, we obtain at 162 K for the concentrations of the dominating aggregates **A**/**B**/**C** the distribution 7 : 81 : 12, characterizing aggregate **B** as the most stable one, in agreement with the results for MeLi/LiBr. In both cases,

aggregates **D** or **E** are minor species with less than 1% contribution. Spectra recorded for different mixing ratios, shown in *Fig. 3,a–c*, yield, with an excess of BuLi, only signals for **A** and **B**, and with an excess of LiBr, aside from a strong signal for $(LiBr)_n$, only signals for **B** and **C**. The constant intensity ratios found for signals *5*/*6* and *3*/*4* give independent support for our signal assignment. Furthermore, spectra recorded at higher temperature reveal coalescences between signals *5* and *6* as well as *3* and *4* (*Fig. 4*). These must be due to an increase of the rate of *intra*-aggregate exchange now also in clusters **B** and **C**. For the exchange system $3 \rightleftharpoons 4$ with equal populations at the two sites, we can calculate the rate constant k at the coalescence temperature T_c (191 K), $k_{coal.}$, from *Eqn. 2* [18] and the chemical shift difference, $\delta\nu$ (in Hz), measured at low temperature:

$$k_{coal.} = \pi \cdot \delta\nu/\sqrt{2} = 2.22\ \delta\nu \tag{2}$$

With $\delta\nu = 0.29$ ppm or 17 Hz at 58.9 MHz from *Table 1*, we find $k_{coal.} = 38\ s^{-1}$; this leads with

$$\Delta G^{\ddagger}_{T_c} = RT_c[22.96 + \ln(T_c/\delta\nu)] \tag{3}$$

and $R = 8.31\ J\ K^{-1}$ to a free energy of activation of $\Delta G^{\ddagger}_{191} = 40.4\ kJ\ mol^{-1}$. The coalescence temperature for signals *5* and *6* is with 200 K slightly higher, but the chemical shift difference is only 0.7 Hz. This gives a $\Delta G^{\ddagger}_{206}$ value of *ca.* 49 kJ mol^{-1} as a crude estimate based on *Eqn. 2*[3]). For cluster **A**, on the other hand, at 162 K still

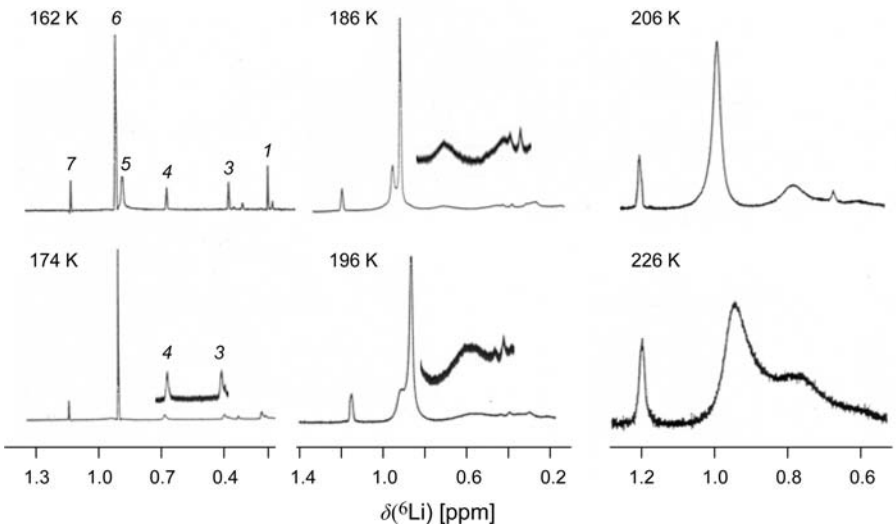

Fig. 4. *Temperature dependence of the* $^6Li\{^1H\}$*-NMR spectrum of* Fig. 2, a. Please note that, for signals *5* and *6*, a temperature-dependent change of the relative chemical shift with an isochrony at 174 K exists.

[3]) *Eqn. 2* is strictly valid only for a two-sites exchange system with equal populations.

characterized as a *fluxional* tetramer, the barrier must be lower. As an upper limit, we estimate on the basis of *Eqn. 2* from the isotope effect of 8.5 ppb, which is only 0.5 Hz for $\delta\nu$ at 58.9 MHz, a $k_{coal.}$ value of *ca.* 1 s^{-1}. This gives $\Delta G^{\neq}_{T_c} < 38.7$ kJ mol^{-1} for the transitions static $\rightleftharpoons$ *fluxional*. At temperatures above 206 K, the beginning coalescence between the signals for clusters **B** and **C** indicates the inset of *inter*-aggregate exchange.

Turning now to the ^{13}C-NMR results for the basic mixture Bu^{6}Li/^{6}LiBr (1.0 : 0.8) in Et_2O, we find at 184 K a distorted *multiplet* at $\delta(^{13}C)$ 11.9 ppm that shows a ^{6}Li,^{13}C coupling constant of 5.5 Hz and a strongly broadened signal around $\delta(^{13}C)$ 11 (*Fig. 5, a*). That indicates, after *Eqn. 1*, the presence of a static tetramer with three $^6Li^+$ ions as the next neighbor environment for $^{13}C(\alpha)H_2$ of the BuLi groups but leaves the origin of the remaining ^{13}C resonances unclear. The *multiplet* could thus originate from cluster **A** (3 × Li-1), **B** (1 × Li-2, 2 × Li-3), or **C** (2 × Li-4, 1 × Li-5). This is most clearly documented by the heteronuclear *Overhauser* effects between ^{6}Li- and the H-atoms of the α-CH_2 group found in the HOESY spectrum [2d][19] of the 1.0 : 0.2 mixture (*Fig. 6, a*) where, according to the spectrum shown in *Fig. 3,a*, the aggregates **A** and **B** dominate. Cross-peaks for **C** could not be observed due to the low intenstity of the Li-4 and Li-5 signals.

A more detailed analysis of the ^{13}C-NMR signals was possible when the ^{13}C spectra of the samples with different ratios [Buli]/[LiBr] were recorded under ^{1}H as well as ^{6}Li decoupling that removes line-broadening due to resolved and unresolved coupling constants (*Fig. 5, b – d*). Accordingly, sharp *singlet*s are observed for the resonances of the lithiated C-atoms at 11.9, 11.7, and 10.9 ppm, because the next neighbor environment for the Bu groups, [Li,Li,Li], is identical within the clusters **A**, **B**, and **C**. The assignment can be based on the intensities observed for the same mixtures as those used in the ^{6}Li-NMR spectrum (*Fig. 3*). The 1.0 : 0.2 mixture (*Fig. 5, b*) with [**B**] > [**A**] gives resonances at $\delta(^{13}C)$ 11.9 for **B** and $\delta(^{13}C)$ 10.9 for **A**, while, for the 1.0 : 2.0 mixture

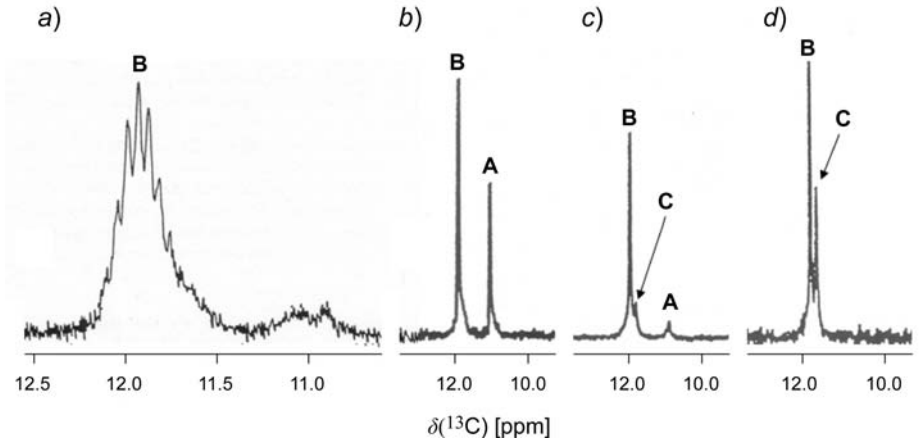

Fig. 5. a) *100-MHz $^{13}C\{^1H\}$-NMR Spectrum of Bu^{6}Li/^{6}LiBr* (1.0 : 0.8) *0.44*M *in Et_2O/[D_{10}]Et_2O 4 : 1 at 184 K*. δ in ppm relative to TMS. b) – d) *Partial $^{13}C\{^1H,^6Li\}$ NMR spectra of samples with different mixing ratios for Bu^{6}Li and ^{6}LiBr at 194 K:* b) *1.0 : 0.2,* c) *1.0 : 0.8,* d) *1.0 : 2.0*.

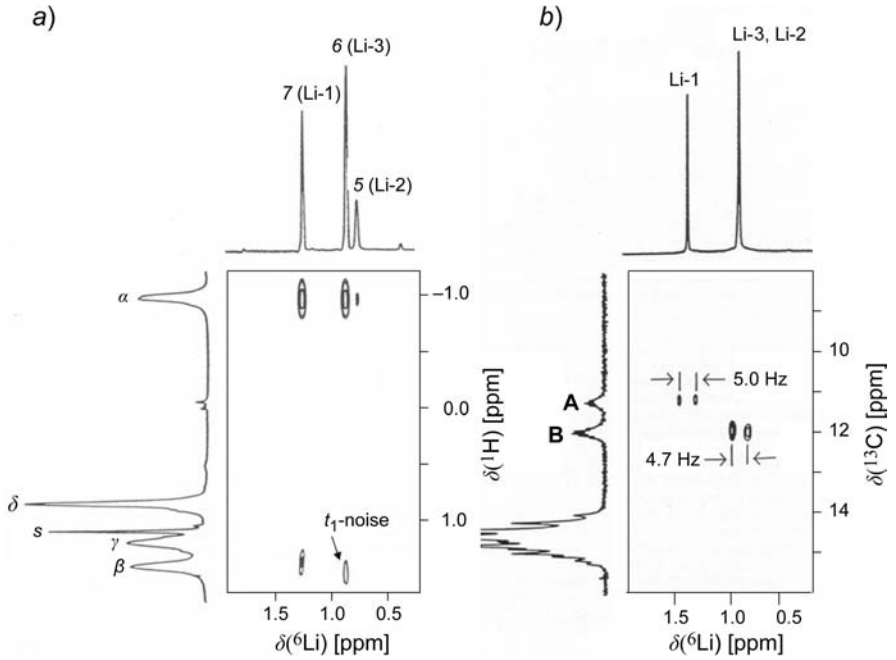

Fig. 6. a) *400/58.9-MHz $^{1}H,^{6}Li$-HOESY Spectrum of Bu^{6}Li/^{6}LiBr* (1.0 : 0.2) *0.7*M *in [D_{10}]Et_2O at 164 K with cross-peaks between ^{1}H–C(α) of the Bu groups and Li-1 in cluster* **A**, *and Li-3 and Li-2 in cluster* **B**. The ^{1}H-NMR signals of the H-atoms of the Bu groups of different clusters are not separated, the known cross-peak between ^{6}Li and the CH_2 H-atoms at C(β) [19] is seen for cluster **A**; *s*, residual Et_2O. b) *Phase-sensitive $^{6}Li,^{13}C$-HMQC spectrum of the same mixture at 174 K*. Please note that, at this temperature, the signals *5* and *6* for Li-2 and Li-3 in cluster **B**, respectively, coincide (see also *Fig. 4* for the temperature dependence of these signals).

with ^{6}Li resonances for **B** and **C**, we observe the ^{13}C signals again at $\delta(^{13}C)$ 11.9 for **B** and now at $\delta(^{13}C)$ 11.7 for **C** (*Fig. 5, d*). For the 1.0 : 0.8 mixture, all three ^{13}C signals are recorded (*Fig. 5, c*). The line splitting of 5.5 Hz observed in the distorted *multiplet* of *Fig. 5, a* (*cf.* above) thus comes from C(α)-atoms of Bu groups of clusters **B** and **C** and their next neighbor environments [Li-2,Li-3,Li-3] and [L-4,L-4,Li-5], respectively. The small broadened signal around $\delta(^{13}C)$ 11, on the other hand, with unresolved coupling is identified as belonging to cluster **A**. The remaining resonances of BuLi were found between 31 and 34 ppm (C(2), C(3)) but not assigned; the C(4) signal was superimposed by solvent signals. As one sees, the influence of Br^- inclusion on $\delta(^{13}C)$ of the lithiated C-atom is small and apparently not systematic.

Further important information for the analysis of the ^{13}C signals was derived from a two-dimensional $^{6}Li,^{13}C$ chemical shift-correlation experiment of the HMQC type [20] for the 1.0 : 0.2 mixture at 194 K, where the signals *5* and *6* of cluster **B** overlap, and the higher intensity of signal *7* allows a closer look on its structure. This experiment yielded $^{13}C,^{6}Li$ cross-peaks with splittings of 5.0 Hz for cluster **A** and 4.7 Hz for cluster **B** (*Fig. 6, b*). According to *Eqn. 1*, cluster **A** is static on the time-scale of this experiment (17 : 5.0 = 3.4) with three $^{6}Li,^{13}C$ contacts. The observed coupling constant agrees with

earlier results for the aggregation state of BuLi in Et_2O [21] that showed at 203 K a $^{13}C,^{7}Li$ coupling of 14 Hz again typical for a static tetramer[4]).

For cluster **B**, we find $n = 3.6$ which is a border case between static ($n = 3$) and *fluxional* ($n = 4$). However, considering the approximate nature of *Eqn. 1*, a static cluster **B** is most likely, because the isotopic fingerprints (*Fig. 3, b*) characterize **B** as static and the signal overlap *5*/*6* and low digital resolution (0.18 Hz) in the HMQC spectrum may cause a larger experimental error for the coupling.

An additional point of interest concerns our finding that the isotopic fingerprint for signal *7* and its aggregate at 162 K are typical for a *fluxional* aggregate (*Fig. 2, b*). This contrasts with the conclusions drawn above from the $^{13}C,^{6}Li$ coupling. The different result of the two recordings is a consequence of the different NMR time-scale that governs the coalescence or decoalescence behavior of the appropriate *multiplet*s. The couplings of 5.0 or 14 Hz must be compared with the isotope effect of only 0.5 Hz. This leads, according to *Eqn. 2*, to the decoalescence of the appropriate signals k values of 11 or 31 s^{-1} and 1 s^{-1}, respectively, for the two experiments with different NMR parameters. A static situation with Li scalar coupled to only three next $^{13}CH_2$ neighbors in the BuLi tetramer, *i.e.*, the slow exchange region for the *intra*-aggregate exchange, is thus reached in the ^{13}C spectrum at higher temperatures. For the chemical shift *multiplet* of the isotopic fingerprint the *intra*-aggregate exchange is still fast enough to average the isotope effect with next and remote neighbors. Only at lower temperatures, that means smaller k values, a static situation can be reached, and the fingerprint *quintuplet* is then transformed into a *quadruplet*. Such a situation was found in our study of the aggregation of BuLi in dimethoxymethane [22]. The labels '*static*' and '*fluxional*' are thus clearly related to the time-scale of the particular NMR experiment.

BuLi/LiBr and TMEDA in Et_2O. The strong coordination tendency of the bidentate diamine ligand TMEDA drastically changes the situation for the aggregation of lithium organics. This is clear from the ^{6}Li-NMR spectrum of $Bu^{6}Li/^{6}LiBr$ (1 : 1) in Et_2O in the presence of an excess of TMEDA (1.5 times the concentration of both lithium compounds) (*Fig. 7, a*). At 175 K, we observe a strong *singlet* at 1.57 ppm and for the partially deuterated mixture $Bu^{6}Li/n\text{-}\alpha,\alpha[D_2]Bu^{6}Li/^{6}LiBr(1:1:2)$/TMEDA a *doublet* as isotopic fingerprint (*Fig. 7, b*). Accordingly, $Bu^{6}Li$ and $^{6}LiBr$ form under these conditions a dimer (**E** in *Fig. 1*). The dimer structure of the BuLi/LiBr/TMEDA cluster is supported by the *quintuplet* at $\delta(^{13}C)$ 12.1 and a coupling of 9.3 Hz found for the lithiated C-atom in the ^{13}C-NMR spectrum of the same sample (*Fig. 7, c*). Not unexpectedly, the strongly solvating diamine prevents tetramer formation completely, but also stabilizes the mixed dimer to the extent that a BuLi homodimer could not be detected.

BuLi/$LiClO_4$ in Et_2O. Aside from lithium halogenides, the aggregation of lithium organics was frequently studied in the presence of other Li salts like $LiClO_4$ that forms in Et_2O a solvent-seperated ion pair, $Li^{+}(Et_2O)_xClO_4^{-}$ ($x = 1, 2$) [23][24]. We found that for the aggregation behavior of MeLi in the presence of $LiClO_4$ different results were reported. While *Ashby et al.* did not find a mixed aggregate [25], a static aggregate

---

[4]) The magnetogyric ratio, γ, of ^{7}Li is larger than that of ^{6}Li by a factor of 2.64 that also holds for the ratio of the coupling constants. *Eqn. 1* than changes to $^{1}J(^{13}C,^{7}Li) \approx 45/n$.

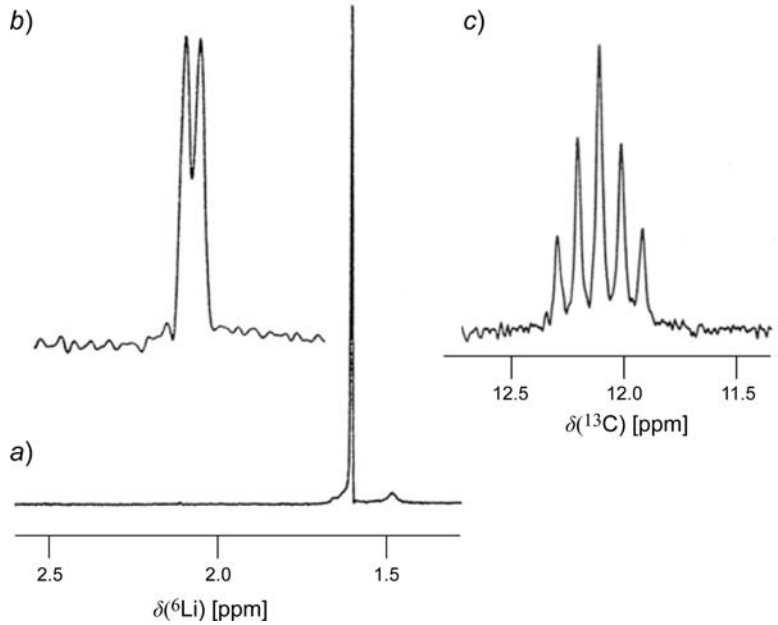

Fig. 7. a) *58.9-MHz ^{6}Li{^{1}H}-NMR Spectrum of Bu^{6}Li/^{6}LiBr/TMEDA* (1:1:1.5) *0.35*M *in [D_{10}]Et$_2$O at 175 K*. δ-Scale relative to external LiBr 0.1M in [D_8]THF. b) *^{6}Li Isotopic fingerprint for Bu^{6}Li/[α,α-D_2]Bu^{6}Li/LiBr/TMEDA* 1:1:2:1.5. c) *^{1}H-Decoupled ^{13}C-NMR signal of the sample used for* a *at 190 K*; δ-scale relative to TMS.

[$Li_4Me_3(ClO_4)$] in the presence of a MeLi tetramer was proposed by *Jackman et al.* [26] and an experiment with BuLi was, therefore, of interest.

The ^{6}Li-NMR spectrum of a 1:1 mixture Bu^{6}Li/^{6}LiClO$_4$ in Et$_2$O showed, relative to the LiBr standard, two *singlet*s at 1.24 and -1.18 ppm. In the isotopic fingerprint spectrum at 173 K, the high-frequency *singlet* changed to a *quintuplet* that characterizes a *fluxional* tetramer of BuLi. The other signal showed no splitting and was assigned to ^{6}LiClO$_4$. Thus, no indication of mixed aggregate formation with BuLi came from these data. This is further supported by the ^{13}C-NMR spectrum with only one signal of a lithiated C-atom at 10.7 ppm, typical for (BuLi)$_4$ as seen in *Fig. 5, b*, for cluster **A** and as reported in [21].

BuLi/PhLi (1:1) *and TMEDA in Et$_2$O.* In addition to the aggregation of organolithium compounds with inorganic salts, aggregation between two lithium organics was repeatedly explored. Again, pioneering work was accomplished by *Seitz* and *Brown*, who reported, among other projects, on mixtures of MeLi and EtLi [16] or MeLi and PhLi in Et$_2$O [27]. Later, for example, BuLi/PhC≡CLi [28a], 1-lithionaphthalene/MeLi [19] or 1-[(dimethylamino)methyl]-2,4,6-trimethylbenzene/BuLi [28b] and, more recently, MeLi/BuLi [28c], $Me_2NC_6H_4Li$/*t*-BuLi [28d], and lithium amides/PhLi [28e] were investigated. It was also shown that such studies can throw light on the mechanism of lithiation reactions.

Our interest focused on a mixture of BuLi and PhLi, two of the most frequently used lithiation agents in organic synthesis. *Seitz* and *Brown* investigated PhLi mixtures

with MeLi and EtLi in Et_2O, and proposed the presence of two mixed species, a dimer, $Li_2(Ph)(Et)$, and a tetramer, $Li_4(Ph)Et_3$ [27]. In the presence of TMEDA, we can expect, according to earlier results for BuLi and PhLi solutions in various solvents [2f][5a][12], the exclusive formation of the dimers **F**, **G**, and **H** (*Fig. 8*).

In the ^{6}Li-NMR spectrum of a 1:1 mixture BuLi/PhLi in Et_2O in the presence of a slight excess of TMEDA (*Fig. 9, a*), we found three signals *8*, *9*, and *10*. Those at highest and lowest frequency with relative intensities of 1:1 are characterized by their chemical

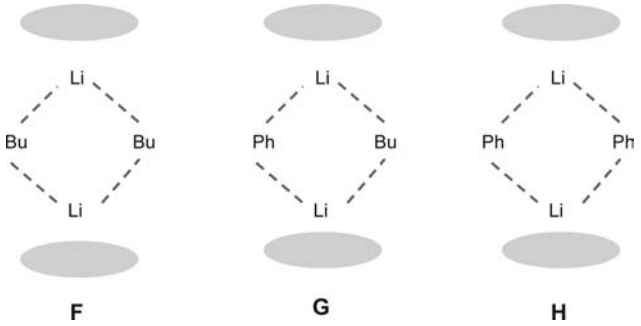

Fig. 8. *Expected dimers for a mixture of BuLi and PhLi in the presence of TMEDA*

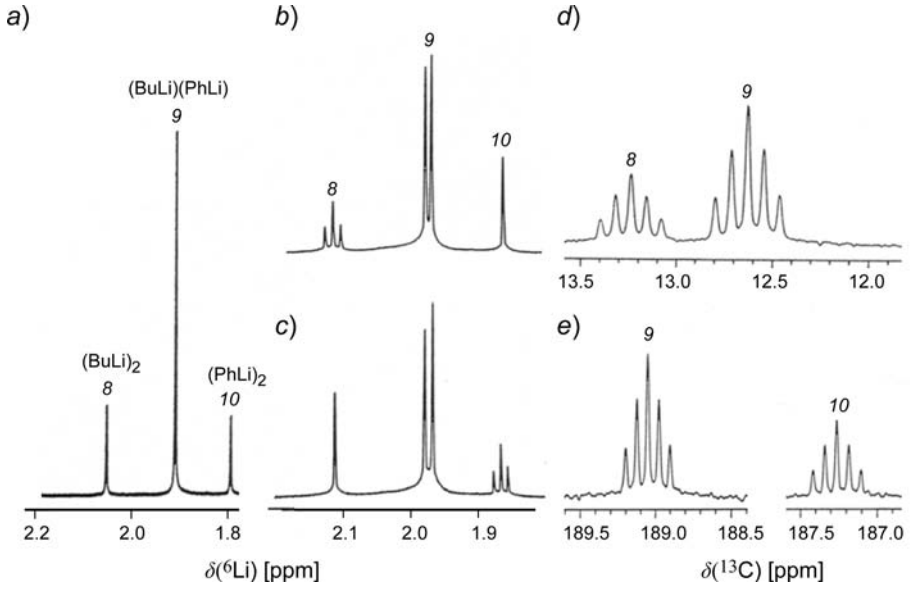

Fig. 9. a) *58.9-MHz ^{6}Li-NMR Spectrum of Bu^{6}Li/Ph^{6}Li* (1:1) *0.3*M *in [D_{10}]Et_2O/TMEDA* ($c_{(TMEDA)}$ 0.7M) *at 185 K*. External standard 0.1M LiBr/[D_8]THF; *8:* $(BuLi)_2(TMEDA)_2$, *9:* $(BuLi)(PhLi)(TMEDA)_2$, *10:* $(PhLi)_2(TMEDA)_2$. b) *Isotopic fingerprints in the ^{6}Li-NMR spectrum of Bu^{6}Li/[α,α-D_2]Bu^{6}Li/Ph^{6}Li* (1:1:2) *0.3*M *in [D_{10}]Et_2O/TMEDA at 188 K*. c) *^{6}Li-NMR Spectrum of Bu^{6}Li/Ph^{6}Li/[D_5]Ph^{6}Li under the same conditions.* d) and e) *100-MHz $^{13}C\{^1H\}$-NMR Spectra of Bu^{6}Li/Ph^{6}Li/TMEDA* (1:1:2.3) *at 200 K in [D_{10}]Et_2O with the signal of C(α) of BuLi and C_{ipso} of PhLi, respectively.* Reference, TMS.

shift values of δ 2.11 and δ 1.86 as belonging to the homodimers of BuLi (**F**) and PhLi (**H**), respectively, each one coordinated with two molecules of TMEDA. This was verified for BuLi by an independent recording in Et_2O in the presence of TMEDA that yielded $\delta(^6Li)$ of 2.16 ppm. The large signal at δ 1.97 of relative intensity 4 is then due to a mixed aggregate **G** of the two organolithium compounds. For an independent proof, isotopic fingerprints were recorded for ^{6}Li-enriched 1:1:2 mixtures of BuLi, [α,α-D_2]BuLi and PhLi as well as for PhLi, [D_5]PhLi and BuLi, both with eqimolar amounts of TMEDA, that resulted in ^{6}Li spectra shown in *Figs. 9, b* and *c*, respectively[5]). From the signal structure, it is immediately clear that only dimers are formed, as expected: *Fig. 9, b* shows the *triplet* for the BuLi dimer **F**, while *Fig. 9, c* displays the *triplet* for the PhLi dimer **H**. The *doublet* in both spectra is due to the mixed dimer **G** where only one ligand provides the isotope shift. We can assume that in all dimers Li is complexed with two molecules of TMEDA. Relevant spectroscopic data are collected in *Table 3*.

Further support for the above results comes from the ^{1}H-NMR spectrum recorded at 200 K where the signals of ^{1}H,^{13}C(α) of the BuLi species and those of the *ortho*-phenyl H-atoms of the PhLi species are doubled in the intensity ratio 1:2. This ratio is the result of the relative intensities of 1:4 of signals *8*/*9* and *10*/*9*. The mixed dimer, however, contains only one unit of BuLi and PhLi, while the homodimers contain two. The assignment was possible through a 2D-^{1}H,^{6}Li HOESY spectrum that yielded cross-peaks for signal *8* with the CH_2 resonance of the dimer $(BuLi)_2$ at $-$1.15 ppm (relative intensity 1) and for signal *9* with that at $-$0.91ppm (relative intensity 2) due to BuLi in the mixed dimer [(BuLi)(PhLi)]. The two signals of *o*-^{1}H of the PhLi species at 7.87 and 8.10 ppm (relative intensity 2:1) correlated with signals *9* and *10*, respectively, and are thus assigned to the mixed dimer and the homodimer $(PhLi)_2$, respectively.

Table 3. *^{6}Li-, ^{13}C-, and ^{1}H-NMR Data for the System BuLi/PhLi* (1:1) *in [D_{10}]Et_2O/TMEDA*

^{6}Li Signal	δ [ppm][a])	Assignment	$^2\Delta(^6Li)$ [ppb][b])	$^n\Delta(^6Li)$ [ppb][c])	Relative intensity
8	2.11	**F**	$-$12.2		0.98
9	1.97	**G**	$-$9.3	$-$11.4	4.00
10	1.86	**H**		$-$10.4	1.01
^{13}C Signal	δ [ppm][d])	$^1J(^{13}C,^6Li)$ [Hz]	^{13}C Signal	δ [ppm][d])	$^1J(^{13}C,^6Li)$ [Hz]
C(α) (**F**)	13.24	8.0 $\pm$ 0.17	C(1) (**G**)	189.05	7.6 $\pm$ 0.17
C(α) (**G**)	12.63	8.4 $\pm$ 0.17	C(1) (**H**)	187.26	7.9 $\pm$ 0.17
^{1}H Signal[e])	δ [ppm][d])	^{1}H Signal[e])	δ [ppm][d])		
^{1}H–C(α) (**F**)	$-$1.15	*o*-^{1}H (**G**)	7.87		
^{1}H–C(α) (**G**)	$-$0.91	*o*-^{1}H (**H**)	8.10		

[a]) Relative to external 0.1M LiBr in THF at 185 K. [b]) ^{1}H/^{2}H isotope shift per CD_2 group. [c]) ^{1}H/^{2}H Isotope shift per C_6D_5 group as sum of *o*-, *m*-, and *p*-shifts. [d]) Relative to TMS at 200 K. [e]) Additional NMR data are given in the *Exper. Part.*

[5]) In the case of (D_5)PhLi, the dominating deuterium induced isotope effect for ^{6}Li is transmitted from the Ph *o*-H-atoms over three bonds as $^3\Delta(^{2/1}H)^6Li$ [29].

It was also of interest to investigate the temperature dependence of the spectra (*Fig. 10*), where coalescence phenomena yield a ^{6}Li average signal at 1.94 ppm. From the coalescence temperatures of *ca*. 235 and 244 K for the equilibria *8* ⇌ *9* and *9* ⇌ *10*, respectively, we estimate with the $\delta\nu$ values of *Fig. 10* and *Eqn. 2 k* values of *ca.* 18 and *ca.* 14 s^{-1} that yield $\Delta G^{\neq}_{coal.}$ values of 51 and 54 kJ mol^{-1} for the *inter*-aggregate exchange systems between the homodimers and the mixed or heterodimer.

The EXSY spectra [30] (*Fig. 11*) confirm the exchange documented in the line-shape changes, but reveal further information of interest. The spectrum measured at 221 K shows, in addition to the cross-peaks between signals *8*/*9* and *9*/*10* that correspond to the signal coalescences in *Fig. 10*, cross-peaks between signals *8* and *10*. If we assume for the exchange processes an association of the dimers to tetramers as intermediates or as transition states, followed by dissociation along different 'cuts' of the tetrameric cube, we can analyze the situation with the help of the aggregates outlined in the *Scheme*. Starting with cluster **I**, formed by homodimer association, $(BuLi)_2/(PhLi)_2$, dissociation along a perpendicular and a horizontal plane leads to an exchange between Li-8 and Li-9, as well as Li-10 and Li-9 (*Path a* and *b*). The same is true if we start with the association of a homo- and a heterodimer (*8* + *9*) and of two heterodimers (*9* + *9*) (not shown in the *Scheme*). A direct Li exchange between the homodimers $(BuLi)_2$ and $(PhLi)_2$, *i.e.*, *8* ⇌ *10*, is thus not possible, if we consider the tetramers as static. In order to realize such an exchange, indicated by the EXSY cross-peaks, we have to assume that tetramer **I** is *fluxional* and Li-8 and Li-10 interchange their position, *i.e.*, **I** → **J**, before dissociation into homodimers (*Path c*). Fluxionality can be expected also for the other tetramers (homodimer + heterodimer and 2 × hetero-dimer), but only tetramer **I** contains both Li species *8* and *10* and allows chemical

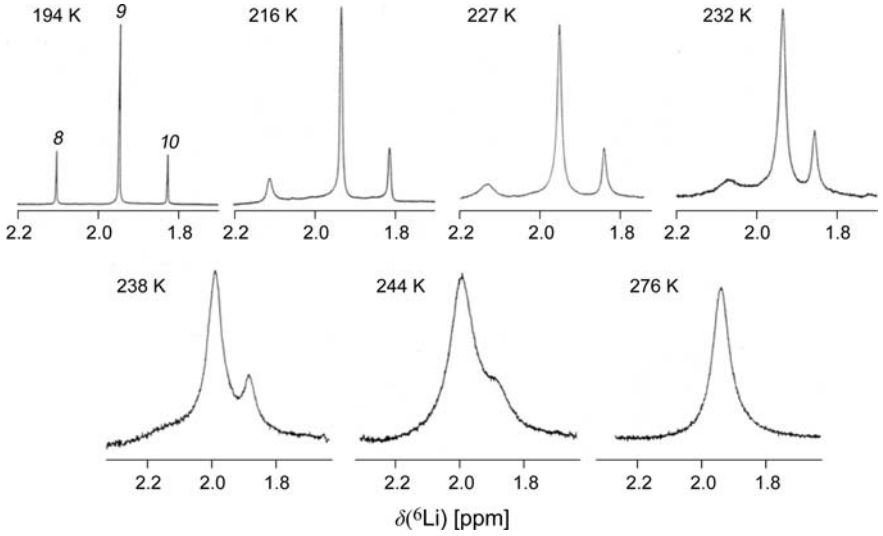

Fig. 10. *Temperature-dependent ^{6}Li-NMR spectra of Bu^{6}Li/Ph^{6}Li* (1:1, 0.3M) *in [D_{10}]Et_2O/TMEDA* (0.7M). $\delta\nu$(*8*/*9*) 8.24 Hz, $\delta\nu$(*9*/*10*) 6.48 Hz, coalescence of signals *8* and *9* is followed by that of *9* and *10* (*8:* $(BuLi)_2(TMEDA)_2$, *9:* $(BuLi)(PhLi)(TMEDA)_2$, *10:* $(PhLi)_2(TMEDA)_2$).

Scheme. *Proposed Association–Dissociation Mechanism for Li Exchange in the BuLi/PhLi/TMEDA Mixture.* The Li sites are indicated by signal numbers as in *Fig. 9*.

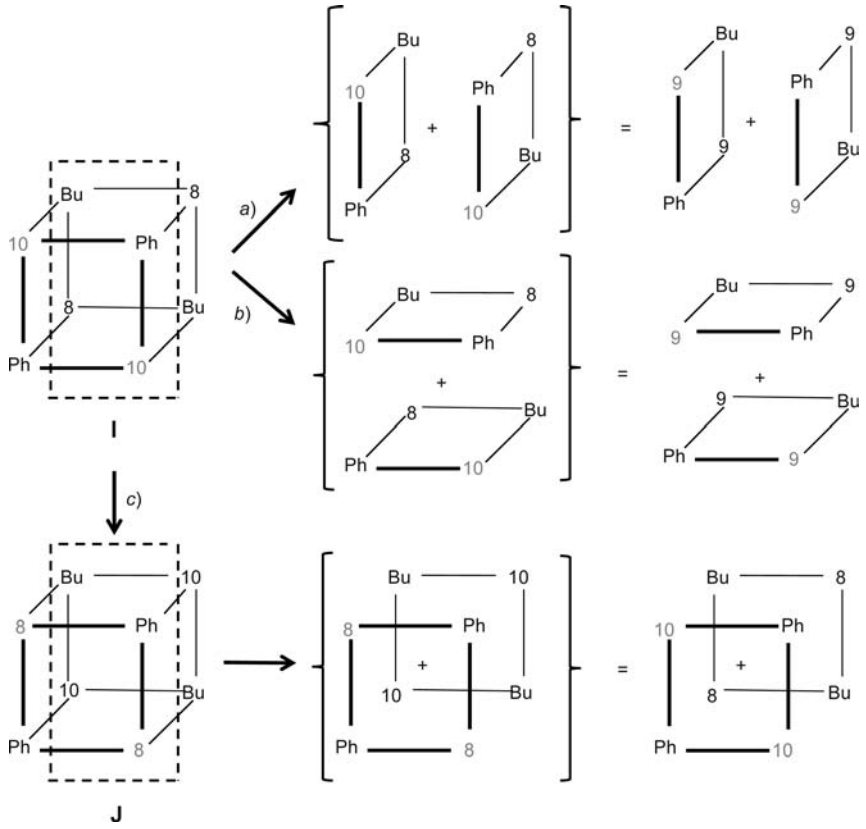

exchange. Consequently, the tetramers are true intermediates with a certain life time for internal Li exchange and not transition states. The larger cross-peak intensity for the exchange systems *8*/*9* and *9*/*10* as compared to that of *8*/*10* supports this mechanism because of the higher concentration of mixed aggregates (*cf.* signal *9 vs. 8* or *10*) the probability for these exchanges is larger. The cross-peaks for *8*/*10* disappear already at slightly higher temperature (227 K), when the slow exchange region for the Li exchange is over because of the higher reaction rate that results, according to *Eqn. 2*, from the larger chemical-shift difference (k of *ca.* 36 *vs.* 18 or 14 s^{-1}).

Discussions. – For the BuLi/LiBr system, we find aggregates like those described earlier for the MeLi/LiBr system [10][11]: $(LiR)_4$ (**A**), Li_4R_3Br (**B**), $Li_4R_2Br_2$ (**C**), Li_4RBr_3 (**D**) and/or Li_2RBr (**E**) (*Fig. 1*). Also the relative abundance of the dominating species is not very different with **A**/**B**/**C** 7 : 81 : 12 in the present case and 7 : 66 : 27 for MeLi/LiBr, and does not follow a statistical distribution. In both systems, cluster **B** is the most stable one, **D** and/or **E** are minor components. A notable difference concerns the ^{6}Li chemical shift which changes systematically in the MeLi/

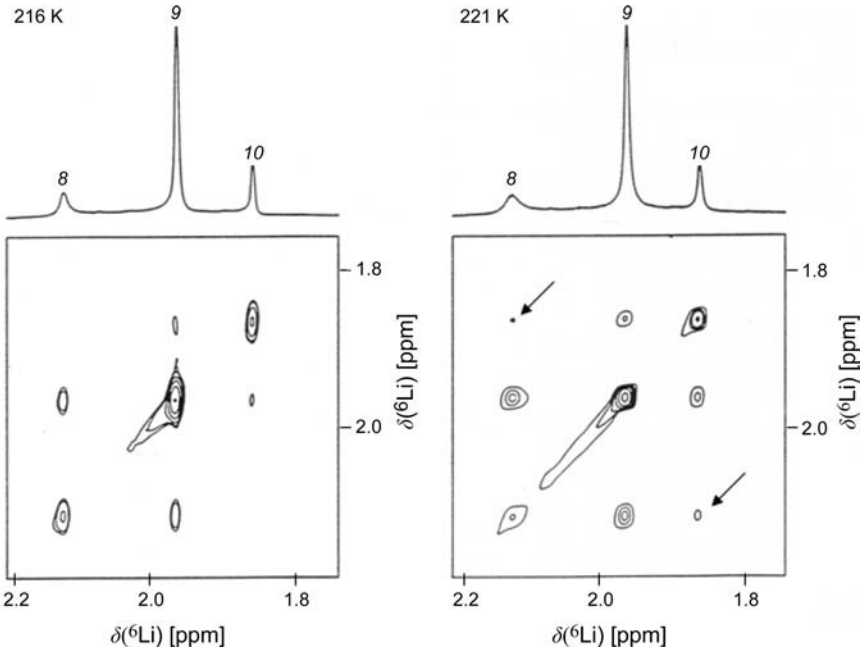

Fig. 11. *2D ^{6}Li,^{6}Li-EXSY Spectra of Bu^{6}Li/Ph^{6}Li* (1:1, 0.3M) *in [D_{10}]Et$_2$O/TMEDA* (0.7M) (*8*: $(BuLi)_2(TMEDA)_2$, *9*: (BuLi)(PhLi)$(TMEDA)_2$, *10*: $(PhLi)_2(TMEDA)_2$)

LiBr system with increased shielding of *ca*. 0.6 ppm for the successive introduction of bromide in the next neighbor environments: $[(Me)_3]$ – $[(Me)_2Br]$ – $[MeBr_2]$. In the case of BuLi/LiBr, $\delta(^{6}Li)$ of the environment $[(Bu)_3]$ that exists for Li-1 and Li-2 in clusters **A** and **B**, respectively, differs by 0.25 ppm, and Li-3 of cluster **B** with environment $[(Bu)_2Br]$ is even deshielded by 0.04 ppm relative to Li-2 with $[(Bu)_3]$. More reasonable is the chemical-shift difference of 0.29 ppm between Li-4 and Li-5 in cluster **C** with environments $[(Bu)_2Br]$ and $[BuBr_2]$, respectively. Assuming a shielding effect by Br^- ion across the diagonal of the tetrameric cube, the relation $\delta(\text{Li-2}) < \delta(\text{Li-1})$ can be understood, as well as the relation $\delta(\text{Li-4}) < \delta(\text{Li-3})$. Li-5 is then shielded by a directly attached second Br^- ion. If Li-6 resides in cluster **D**, one would then expect a shielding effect from the Br^- ion across the diagonal and the relation $\delta(\text{Li-6}) < \delta(\text{Li-5})$. The small shift difference of only 0.03 ppm does not support the presence of this shielding mechanism, and the existence of the mixed dimer **E** is more likely. The mechanism of the cross-diagonal shielding is unclear. Certainly, the larger alkyl group in BuLi as compared to MeLi causes severe distortions of the tetramer structure that might involve hitherto unknown shielding effects. That aggregation of organolithium compounds may yield unexpected results was recently shown by studies of MeLi in THF in the presence of LiCl, where *Maddaluno* and co-workers found, aside from the tetramer $(MeLi)_4$ and the dimer $(LiCl)_2$, exclusively a mixed dimer (MeLi)(LiCl) of type **E** [31]. This indicates for the MeLi/lithium halogenide 1:1 mixtures in THF as solvent a decrease in the number of mixed aggregates in the order LiI > LiBr > LiCl from 3 (**B**, **C**, and **E**) to 2 (**B** and **E**) to 1 (**E**). In the same order, the proportion

of the homo-aggregate $(LiMe)_4$ decreases, and that of the heterodimer **E** increases. Evidence for the existence of tetramer **D** comes only from samples with an excess of LiX[6]).

It is interesting to compare the free activation barriers that we calculated from the temperature-dependent ^{6}Li spectra for the *intra*-aggregate or *fluxional* exchange in aggregates **A**, **B**, and **C** with data published by *Thomas* and coworkers for *fluxional* exchange in *t*-BuLi and *t*-pentyllithium [32]. For *t*-BuLi one derives from the given $\Delta H^{\neq}$ and $\Delta S^{\neq}$ values of 25 kcal mol^{-1} and 44 cal K^{-1} mol^{-1}, respectively, $\Delta G^{\neq}_{191} = 69$ kJ mol^{-1}. This compares reasonably well with $\Delta G^{\neq}_{191}$ and $\Delta G^{\neq}_{206}$ values 40.4 and 49 kJ mol^{-1} we found for cluster **C** and **B**, respectively. At 162 K, cluster **A**, the tetramer of BuLi, is still *fluxional*, and our estimated barrier of < 38.7 kJ mol^{-1} at coalescence to the static structure at lower temperature comes close to the value of 33 kJ mol^{-1} estimated for *t*-pentyllithium at 188 K [32].

Our finding for the BuLi/PhLi mixture supports the proposal of the formation of a mixed dimer Li_2(Ph,R) in the mixtures of PhLi with MeLi and EtLi, respectively [27]. The presence of TMEDA prevented in our case the formation of a mixed tetramer. Of general interest is the *experimental proof* that the Li exchange between different heterodimers proceeds *via* tetramers formed by dimer association as *intermediates* with a lifetime that allows *intra*-aggregate Li exchange before dissociation.

Again, a mixture of PhLi with alkylithium compounds does not lead to a statistical distribution of the products as was found for mixtures of alkyllithium compounds [16][28c], but shows stabilization of the mixed aggregates. The intensity ratio 1:4:1 for signals *8–10* deviates appreciably from the ratio 1:2:1 expected for a statistic distribution [9] of the two Li compounds. According to *Eqn. 4*, neglecting the coordination of each species with two molecules of TMEDA, we have for the equilibrium constant *K* (*Eqn. 5*) [33], and the mixed dimer is thus more stable than the homodimers by $\Delta G^{\circ}_{185} = -RT \ln K = -4.3$ kJ mol^{-1}:

$$(BuLi)_2 + (PhLi)_2 \rightleftharpoons 2(BuLi,PhLi) \tag{4}$$

$$K = [(BuLi,PhLi)]^2/[(BuLi)_2][(PhLi)_2] = 16 \tag{5}$$

The interconversion barriers $\Delta G^{\neq}_{240}$ of *ca.* 50 kJ mol^{-1} derived above for the *inter*-aggregate homodimer/heterodimer exchange *8*⇌*9* and *9*⇌*10* can be compared with exchange barriers between homotetramers and homodimers. For the dissociation of $(MeLi)_4 \rightarrow 2(MeLi)_2$ in Et_2O $\Delta G^{\neq}_{238} = 48$ kJ mol^{-1} was reported [34] and for the reaction $(BuLi)_4 \rightarrow 2(BuLi)_2$ in THF barrier values of 48 [35] and 46.9 [36] kJ mol^{-1} at 238 K can be calculated from the reported activation parameters. $\Delta G^{\neq}_{238} = 50.4$ resulted for the dimer/tetramer exchange system of vinyllithium [2f]. A much higher barrier of $\Delta G^{\neq}_{302}$ 102 ± 25 kJ mol^{-1} was, however, measured for the dissociation of $(t\text{-BuLi})_4$ in cyclopentane [34b][37]. It seems surprising that these values – except the last one – are comparable to the barriers discussed before for *intra*-aggregate or *fluxional* exchange. This suggests that the free-energy difference between the homodimers and the tetramer

---

[6]) Preliminary investigations for the sytem BuLi/LiI (1:1) in Et_2O show that, aside from cluster **A**, cluster **B** (X = I) is the dominant species (B. Böhler, H. Günther, unpublished).

intermediates of the (BuLi)/(PhLi)/TMEDA system is small, otherwise $\Delta G^{\neq}_{240}$ should be much higher. Alternatively, the barrier to *fluxional* exchange of Li in these tetramer intermediates could be much lower than that in the stable aggregates in order to fit the overall barrier of *ca.* 50 kJ mol^{-1} that also includes the *formation* of the intermediates.

In all cases cited above, the tetramer is a stable, detectable species in contrast to the BuLi/PhLi/TMEDA system where the tetramers are short-lived intermediates that could only indirectly be detected by the EXSY experiment. We can assume that their instability is a consequence of the aggregation with the strong donor TMEDA, as it is known that, for example, BuLi tetramers are destabilized by this ligand [35]. An alternative interpretation follows a proposal made by *T. L. Brown* for the intermediate assumed in the dissociation of *t*-BuLi [34b]: instead of tetramers in the strict sense, the intermediates could be solvent-caged species of the type {$(BuLi)_2(PhLi)_2$}, {$(BuLi)_2$, BuLi, PhLi)}, or {BuLi, PhLi, $(PhLi)_2$}. As a consequence, the barriers of formation and internal Li exchange could be much lower.

For the characterization of minor components of mixtures between organolithium compounds, and metal salts or other additives, the isotopic fingerprint method with deuterated and non-deuterated species, and ^{6}Li enrichment is superior to the use of ^{13}C spectroscopy and ^{13}C,^{6}Li coupling constants, because the nucleus of high natural abundance is measured, and ^{6}Li labelling clearly does not suffer from the difficulties of ^{13}C labelling. Deuteration of the ligands is generally easy to achieve. The EXSY results for the BuLi/Phli mixture demonstrate again the advantage of the 2D over the 1D method, because in 1D spectra small exchange systems like *8* $\rightleftharpoons$ *10* may be completely masked by the exchange broadening of the larger lines.

We are indebted to Prof. Dr. *A. Maercker* for helpful comments, and to the *Fonds der Chemischen Industrie*, Frankfurt, for financial support.

Experimental Part

General. Butyl(Li^6)lithium was prepared as hexane soln. from 1-chlorobutane by a standard procedure [5a] with commercially available ^{6}Li. (α,α-D_2)[^{6}Li]butyllithium was synthesized by the same procedure from 1,1-(D_2)butan-ol *via* 1-chloro[1,1-D_2]butane, available as described [38]. For the isotopic fingerprint measurements the mixtures of deuterated and non-deuterated BuLi were directly prepared from the appropriate mixtures of deuterated and non-deuterated chlorobutane. *Gilman* titrations [39] were used to determine the concentrations. The synthesis of ^{6}Li enriched LiBr and $LiClO_4$ from LiOH and Li_2CO_3, resp., was accomplished as described in [40]. Salt-free PhLi was prepared according to [41], and for the partially deuterated samples we used bromobenzene/bromo[D_5]benzene (1:1) as starting materials as described in [2f].

The NMR tubes (5 mm) were carefully dried on the vacuum line and filled under Ar with the hexane solns. of the Li compounds and the appropriate amount of Li salts or TMEDA dissolved under Ar in O_2-free Et_2O, dried over Li[AlH_4]. The solvents were evaporated on the vacuum line from the frozen samples (acetone/liquid N_2) and then replaced at r.t. by the necessary amount of Et_2O/[D_{10}]Et_2O (4:1). After freezing again at liquid N_2 temp., the NMR tubes were sealed under vacuum.

Spectra. The NMR spectra were recorded with a *Bruker 400* MHz NMR spectrometer with frequencies of 400.13, 100.62, and 58.88 MHz for ^{1}H, ^{13}C, and ^{6}Li, resp. The MLEV-16 sequence [42] was used for ^{1}H broadband decoupling. For the 2D and triple-resonance experiments a ^{1}H,^{13}C,BB triple resonance probehead with appropriate frequency filters was employed. The *Bruker* low-temp. unit was used for variable-temp. spectra, and the temps. were measured with the MeOH thermometer. The ^{1}H- and ^{13}C spectra were referenced to Me_4Si, ^{6}Li spectra to 0.1M LiBr in [D_8]THF as external reference.

Additional ^{1}H-NMR data determined for the BuLi/PhLi mixture by a 2D-COSY-45 [43] experiment and not given in *Table 3* are for the BuLi homodimer H_{β} 1.51, H_{γ} 1.20, H_{δ} 0.85 ppm and for the mixed dimer H_{β} 1.67, H_{γ} 1.30, H_{δ} 0.91 ppm; for the PhLi homodimer *m*-H 6.96, *p*-H 6.85 ppm and for the mixed dimer *m*-H 6.87, *p*-H 6.78 ppm. Spectral parameters: ^{6}Li,^{1}H 2D-HOESY: SW 2551 Hz (F_1), 166 Hz (F_2), 22 × 64 scans, mixing time 1.5 s, exp. time 2.3 h; ^{6}Li,^{13}C 2D-HMQC: SW 1008 Hz (F_1), 177 Hz (F_2), 32 × 128 scans, preparation delay 85 ms, exp. time 7.8 h; ^{6}Li,^{6}Li 2D-EXSY: sweep width, 58.9 Hz (F_1 and F_2), 64 t_1 increments with 32 scans; mixing time, 1 s, time of experiment, 4.9 h. The isotopic fingerprint method [6] rests on the secondary D-induced isotope shift that yields for 1:1 mixtures of non-deuterated (h) and deuterated (d) ligands ^{6}Li-NMR signals in the environment LiR as 1:1 *doublet* (R = h or d), in the environment LiR_2 as 1:2:1 *triplet* (R_2 = hh, (hd, dh), dd), in the environment LiR_3 as 1:3:3:1 *quadruplet* (R_3 = hhh, (hhd, hdh, dhh), (hdd, dhd, ddh), ddd), and in the environment LiR_4 as *quintuplet* 1:4:6:4:1 (R_4 = hhhh, (hhhd, hhdh, hdhh, dhhh), (hhdd, hdhd, hddh, dhhd, dhdh, ddhh), (hddd, dhdd, ddhd, dddh), dddd).

REFERENCES

[1] K. Bergander, D. Hüls, S. J. Glaser, H. Günther, B. Luy, *Magn. Reson. Chem*. **2014**, *52*, 739.

[2] a) J. B. Grutzner, 'Application of NMR in Carbanion Chemistry', in 'Encyclopedia of Nuclear Magnetic Resonance', Eds. D. M. Grant and R. K. Harris, John Wiley & Sons, Ltd, Chichester, 2002, Vol. 9, p. 481; b) H. Günther, 'High-resolution ^{6,7}Li-NMR of organolithium compounds', in 'Encyclopedia of Nuclear Magnetic Resonance', Eds. D. M. Grant and R. K. Harris, John Wiley & Sons, Ltd., Chichester, 1996, Vol. 5, p. 2807; c) H. Günther, '*High resolution ^{6,7}Li-NMR of organolithium compounds*', in 'Advanced Applications of NMR to Organometallic Chemistry', Eds. M. Gielen, R. Willem, B. Wrackmeyer, Wiley-VCH Verlag GmbH, Weinheim, 1996, p. 247; d) W. Bauer, 'NMR of Organolithium Compounds: General Aspects and Application of Two-Dimensional Heteronuclear Overhauser Effect Spectroscopy (HOESY)' in 'Lithium Chemistry – a Theoretical and Experimental Overview', Eds. A.-M. Saspe, P. v. R. Schleyer, John Wiley & Sons, Chichester 1995, p. 125; e) H. Günther, D. Moskau, P. Bast, D. Schmalz, *Angew. Chem*. **1987**, *99*, 1242; *Angew. Chem.*, *Int. Ed.* **1987**, *26*, 1212; f) G. Fraenkel, H. Hsu, B. M. Su, in 'Lithium: Current Applications in Science, Medicine, and Technology', Ed. R. O. Bach, John Wiley & Sons, New York, 1985, p. 273; g) J. L. Wardell, 'Alkali Metals', in 'Comprehensive Organometallic Chemistry', Vol. 1, Eds. G. Wilkinson, F. G. A. Stone, E. W. Abel, Pergamon Press, Oxford 1982, p. 43.

[3] W. Bauer, D. Seebach, *Helv. Chim. Acta* **1984**, *67*, 1972.

[4] G. Fraenkel, M. Henrichs, J. M. Hewitt, B. M. Su, M. J. Geckle, *J. Am. Chem. Soc*. **1980**, *102*, 3345.

[5] a) D. Seebach, R. Hässig, J. Gabriel, *Helv. Chim. Acta* **1983**, *66*, 308; b) W. Bauer, W. R. Winchester, P. v. R. Schleyer, *Organometallics* **1987**, *6*, 2371.

[6] O. Eppers, H. Günther, *Helv. Chim. Acta* **1990**, *73*, 2071; H. Günther, *J. Braz. Chem. Soc.* **1999**, *10*, 241.

[7] I. Keresztes, P. G. Williard, *J. Am. Chem. Soc*. **2000**, *122*, 10228; D. Li, I. Keresztes, R. Hopson, P. G. Williard, *Acc. Chem. Res.* ***2009***, *42*, 270; C. Su, R. Hopson, P. G. Williard, *Eur. J. Inorg. Chem*. **2013**, 4136; G. Hamdoun, M. Sebban, E. Cossoul, A. Harrison-Marchand, J. Maddaluno, H. Oulyadi, *Chem. Commun.* **2014**, *50*, 4073.

[8] R. B. Bates, C. A. Ogle, 'Carbanion Chemistry', Springer Verlag, Berlin, 1984.

[9] D. P. Novak, D. L. Brown, *J. Am. Chem. Soc.* **1972**, *94*, 3793.

[10] T. Fox, H. Hausmann, H. Günther, *Magn. Reson. Chem*. **2004**, *42*, 788.

[11] S. Desjardins, K. Flinois, H. Oulyadi, D. Davoust, C. Giessner-Prettre, O. Parisel, J. Maddaluno, *Organometallics* **2003**, *22*, 4090.

[12] M. Schlosser, 'Struktur und Reaktivität polarer Organometalle', Springer Verlag, Berlin 1973, p. 8.

[13] E. Weiss, E. A. C. Lucken, *J. Organomet. Chem*. **1964**, *2*, 197; E. Weiss, C. Henken, *J. Organomet. Chem*. **1970**, *21*, 256.

[14] T. V. Talalaeva, A. N. Rodinov, K. A. Kocheshkov, *Dokl. Akad. Nauk. SSSR* **1964**, *154*, 174.

[15] R. Freeman, H. D. W. Hill, R. Kaptein, *J. Magn. Reson*. **1972**, *7*, 327; S. Braun, H.-O. Kalinowski, S. Berger, '150 and More Basic NMR Experiments', Wiley-VCH, Weinheim, 1998, p. 123, 298; H. Günther, 'NMR Spectroscopy', 3rd edn., Wiley-VCH, Weinheim 2013, p. 382.
[16] L. M. Seitz, T. L. Brown, *J. Am. Chem. Soc*. **1966**, *88*, 2174.
[17] K. Seidmann, G. E. Maciel, *J. Am. Chem. Soc*. **1977**, *99*, 659, and refs. cit. therein; H. Günther, 'NMR Spectroscopy', 3rd edn., Wiley-VCH, Weinheim 2013, p. 409.
[18] H. S. Gutowsky, C. H. Holm, *J. Chem. Phys.* **1956**, 25, 1228; H. Günther, 'NMR Spectroscopy', 3rd edn., Wiley-VCH, Weinheim 2013, p. 509.
[19] W. Bauer, T. Clark, P. v. R. Schleyer, *J. Am. Chem. Soc*. **1987**, *109*, 970.
[20] L. Müller, *J. Am. Chem. Soc*. **1979**, *101*, 4481; A. Bax, R. H. Griffey, B. L. Hawkins, *J. Magn. Reson*. **1983**, *55*, 301; H. Günther, NMR Spectroscopy, 3rd edn., Wiley-VCH, Weinheim 2013, p. 389.
[21] L. D. McKeever, R. Waack, *Chem. Comm*. **1969**, 750.
[22] K. Bergander, R. He, N. Chandrakumar, O. Eppers, H. Günther, *Tetrahedron* **1994**, *50*, 5861.
[23] Y. Pocker, D. L. Ellsworth, *J. Am. Chem. Soc*. **1977**, *99*, 2276.
[24] D. W. James, R. E. Mayes, *Aust. J. Chem*. **1982**, *35*, 1785.
[25] E. C. Ashby, J. J. Lin, J. J. Watkins, *Tetrahedron Lett*. **1977**, 1709.
[26] L. M. Jackman, E. F. Rakiewicz, A J. Benesi, *J. Am. Chem. Soc*. **1991**, *113*, 4101.
[27] L. M. Seitz, T. L. Brown, *J. Am. Chem. Soc*. **1967**, *89*, 1607.
[28] a) R. Hässig, D. Seebach, *Helv. Chim. Acta* **1983**, *66*, 2269; b) P. Wijkens, E. M. van Koten, M. D. Janssen, J. T. B. H. Jastrzebski, A. L. Spek, G. van Koten, *Angew. Chem*. **1995**, *107*, 239; *Angew. Chem.*, *Int. Ed.* **1995**, *34*, 219; c) F. Paté, H. Oulyadi, A. Harrison-Marchand, J. Maddaluno, *Organometallics* **2008**, *27*, 3564; d) A.-C. Pöppler, M. M. Meinholz, H. Faßhuber, A. Lange, M. John, D. Stalke, *Organometallics* **2012**, *31*, 42; e) H. Oulyadi, C. Fressigné, Y. Yuan, J. Maddaluno, A. Harrison-Marchand, *Organometallics* **2012**, *31*, 4801.
[29] O. Eppers, H. Günther, *Helv. Chim. Acta* **1992**, *75*, 2553.
[30] J. Jeener, B. H. Meier, P. Bachmann, R. R. Ernst, *J. Chem. Phys.* **1979**, *71*, 4546; H. Günther, 'NMR Spectroscopy', 3rd edn., Wiley-VCH, Weinheim 2013, p. 514.
[31] B. Lecachey, H. Oulyadi, P. Lameiras, A. Harrison-Marchand, H. Gérard, J. Maddaluno, *J. Org. Chem*. **2010**, *75*, 5976.
[32] R. D. Thomas, M. T. Clarke, R. M. Jensen, T. C. Young, *Organometallics* **1986**, *5*, 1851.
[33] H. Ulich, W. Jost, 'Kurzes Lehrbuch der physikalischen Chemie', Steinkopff, Darmstadt 1954, p. 84.
[34] a) K. C. Williams, T. L. Brown, *J. Am. Chem. Soc*. **1966**, *88*, 4134; b) T. L. Brown, *Acc. Chem. Res.* **1968**, *1*, 23.
[35] J. F. McGarrity, C. A. Ogle, *J. Am. Chem. Soc*. **1985**, *107*, 1805.
[36] J. Heinzer, J. F. M. Oth, D. Seebach, *Helv. Chim. Acta* **1985**, *68*, 1848.
[37] M. Y. Darensbourg, B. Y. Kimura, G. E. Hartwell, T. L. Brown, *J. Am. Chem. Soc*. **1970**, *92*, 1236.
[38] 'Autorenkollektiv Organikum', 15th edn., 1977, VEB Dt. Verlag d. Wiss., Berlin.
[39] H. Gilman, F. K. Cartledge, *J. Organomet. Chem*. **1964**, *2*, 447.
[40] J. E. Coates, E. G. Taylor, *J. Chem. Soc*. **1936**, 1245.
[41] G. Wittig, E. Benz, *Chem. Ber.* **1958**, *91*, 873; H. J. S. Winkler, H. Winkler, *J. Am. Chem. Soc*. **1966**, *88*, 964.
[42] M. H. Levitt, R. Freeman, T. Frenkiel, *J. Magn. Reson*. **1982**, *50*, 157.
[43] A. Bax, R. Freeman, *J. Magn. Reson.* **1981**, *44*, 542; H. Günther, 'NMR Spectroscopy', 3rd edn., Wiley-VCH, Weinheim 2013, p. 304.

Received November 20, 2014